Excitation of edge modes in the interaction of electron beams with dielectric wedges

R. Garcia-Molina and A. Gras-Marti
Laboratori de Capes Fines i Cololisions Atòmiques, Departament de Física, Facultat de Ciències, Universitat d'Alacant, Apartat 99, E-03080 Alacant/Alicante, Spain

R. H. Ritchie
Health and Safety Research Division, Oak Ridge National Laboratory, Oak Ridge, Tennessee 37830
(Received 23 May 1984)

Recent experimental data on electron-energy-loss spectrometry of the interaction between small crystallites and beams traveling at a fixed beam-solid surface distance are analyzed in terms of the surface and bulk excitation modes of parabolically shaped wedges. The probability of excitation of the surface modes is calculated, in the nonretarded limit, for an electron traveling parallel to the wedge surface, either outside or inside the dielectric wedge. The main features of available experimental data for MgO crystallites can be explained by the theory.

I. INTRODUCTION

In recently reported experiments with scanning transmission electron microscopes (STEM), Marks,[1] Cowley,[2] and Wheatley *et al.*[3] have measured the spectra of energy losses of electron beams interacting with small crystallites of various oxides (MgO, NiO, Al_2O_3, etc.). Given the complex dielectric function of these materials, one might try to relate the spectrum of surface and bulk excitations that the dielectric is able to sustain, with the spectrum of electron energy losses. The dielectric wedge may sustain surface electromagnetic waves that are localized within the vicinity of the edge, and propagate freely along it.

The novel character of the experiments lies in the attempt to probe the surface plasmon field directly by keeping the electron beam traveling, either internally or externally to the wedge but close to the wedge surface, and at a fixed impact parameter.

The interaction of electron probes with semi-infinite solids has been tackled theoretically.[4] This work is one attempt to analyze the aloof excitation of the surface plasmon field of a solid having a given nonplanar boundary.

The crystallites which are bombarded in the experiments[1,2] are of cubic symmetry, about 20—200 nm in size, and the electron beam is oriented along the principal crystallographic directions. One might try to model these crystallites as sharp-edged wedges.[5] The calculation of the dispersion relations for electrostatic modes of a sharp-edged wedge, neglecting spatial dispersion, is due to Dobrzynsky and Maradudin.[6] They find that the eigenfrequencies are independent of wave number and depend continuously on the separation constant for the Laplace equation. Davis[7] has considered the electrostatic modes of a hyperbolic cylinder and has concluded that the results in Ref. 6 are associated with the sharpness of the edge of the wedge. An effect equivalent to the rounding of the edge of the wedge can also be achieved by using a nonlocal dielectric function.[8]

The mathematical analysis of the sharp-edged wedge is difficult, the functions involved are very cumbersome to deal with, and certain divergences in the fields arise.[7,9] On the other hand, the use of a hyperbolic-wedge cylinder[7] might seem to be a useful model of the experimental situation, since the sharp-edged wedge is its natural limit. However, the mathematical analysis in terms of elliptic cylinder coordinates leads to differential equations which Davis[7] solves numerically.

Due to all these facts, and in order to work with analytical solutions, we shall consider the case of a parabolic wedge, where analytical solutions of the wedge surface modes, both in the nonretarded[10] and retarded[11] limits are available. Although this system does not contain the sharp edge as a limit, it will allow us to draw useful information on the experiment.

We shall calculate the energy-loss function and the excitation probability of the wedge modes, due to a pointlike (δ-function) electron beam passing parallel to the dielectric wedge surface. We shall limit our calculations to the nonretarded limit. The theoretical predictions are then compared with experimental data, and it is shown that the main features of the experiment reported by Marks[1] can be explained by the theory.

II. ENERGY LOSS AND EXCITATION PROBABILITY

Take a dielectric wedge infinite in the z direction, with a parabolic-cylinder boundary. The study of the electrostatic edge modes along a parabolic wedge is due to Eguiluz and Maradudin,[10] who solved Laplace's equation in the appropriate coordinate system. Here we shall only give the main steps in the derivation of the electrostatic potential originated as a result of an electron beam traveling along the wedge surface, and parallel with the edge.

The parabolic cylinder coordinate system is defined by[12]

$$\begin{aligned} x &= \xi\eta, \quad -\infty < \xi < \infty, \ 0 < \eta < \infty \\ y &= \tfrac{1}{2}(\eta^2 - \xi^2), \quad -\infty < \xi < \infty, \ 0 < \eta < \infty \\ z &= z \ . \end{aligned} \tag{1}$$

The dielectric wedge occupies the region $0 \le \eta \le \eta_0$, $-\infty < \xi < \infty$ (see Fig. 1), and is characterized by an isotropic dielectric function $\epsilon(w)$.

We consider first the case of a beam traveling external to the wedge, in vacuum ($\epsilon=1$), with a position defined by $\vec{r}_i=(\xi_i,\eta_i,z_i)$, where $\eta_i > \eta_0$ and $-\infty < \xi_i < \infty$. We solve Poisson's equation for the potential

$$\nabla^2\phi(\vec{r},t) = -4\pi\rho(\vec{r},t) , \tag{2}$$

where the charge density associated with an electron beam, which is described classically by a δ function, and moving in the z direction with a velocity v, is

$$\rho(\vec{r},t) = e\delta(\vec{r}-\vec{r}_i) = \frac{e}{\xi^2+\eta^2}\delta(\xi-\xi_i)\delta(\eta-\eta_i)\delta(z-vt) . \tag{3}$$

e is the electron charge.

It is convenient to work in Fourier space:

$$\phi(\xi,\eta,z,t) = \frac{1}{(2\pi)^2}\int_{-\infty}^{\infty} dw\, e^{-iwt}\int_{-\infty}^{\infty} dq\, e^{iqz}\phi(\xi,\eta,q,w) . \tag{4}$$

Then Poisson's equation becomes, in parabolic-cylinder coordinates, with $\phi=\phi(\xi,\eta,q,w)$,

$$\frac{\partial^2\phi}{\partial\xi^2}+\frac{\partial^2\phi}{\partial\eta^2}-(\xi^2+\eta^2)q^2\phi = \begin{cases} 0, & \eta<\eta_0 \quad (5a) \\ -8\pi^2 e\delta(w-qv)\delta(\xi-\xi_i)\delta(\eta-\eta_i), & \eta>\eta_0 . \quad (5b) \end{cases}$$

The solution for the electrostatic potential inside the dielectric wedge is then

$$\phi^{\text{in}}(\xi,\eta,q,w) = \sum_{n=0}^{\infty} A_n F_n(\xi) V(n+\tfrac{1}{2},\sqrt{2q}\,\eta) \tag{6a}$$

and outside the wedge

$$\phi^{\text{out}} = \phi^{\text{ind}} + \phi^{\text{inhom}} . \tag{6b}$$

ϕ^{inhom}, the particular solution of the inhomogeneous Eq. (5b), is given by

$$\phi^{\text{inhom}}(\xi,\eta,q,w) = \sum_n C_n V(n+\tfrac{1}{2},\sqrt{2q}\,\eta)U(n+\tfrac{1}{2},\sqrt{2q}\,\eta_i)F_n(\xi), \quad \eta<\eta_i \tag{6c}$$

$$= \sum_n C_n V(n+\tfrac{1}{2},\sqrt{2q}\,\eta_i)U(n+\tfrac{1}{2},\sqrt{2q}\,\eta)F_n(\xi), \quad \eta>\eta_i \tag{6d}$$

with

$$C_n = 4\pi^{5/2}q^{-1/2}e\delta(w-qv)F_n(\xi_i) .$$

ϕ^{ind} in Eq. (6b) is the potential acting on the electron due to the wedge (the induced or reaction field),

$$\phi^{\text{ind}}(\xi,\eta,q,w) = \sum_n B_n F_n(\xi) U(n+\tfrac{1}{2},\sqrt{2q}\,\eta) . \tag{6e}$$

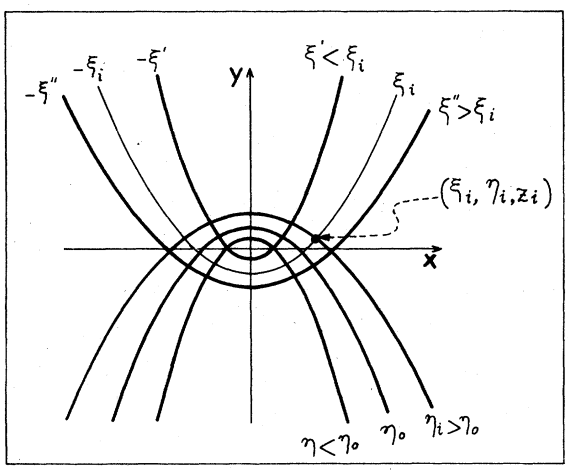

FIG. 1. Parabolic-cylinder coordinates. The parabola $y=\frac{1}{2}(-x^2/\eta_0^2+\eta_0^2)$ defines the dielectric wedge. The wedge occupies the region $\eta<\eta_0$, and the beam travels either in vacuum ($\eta>\eta_0$) or through the wedge ($\eta<\eta_0$), through the point (ξ_i,η_i,z_i).

U and V are parabolic-cylinder functions,[13] and the function $F_n(\xi)$ contains the Hermite polynomial[13] of nth order $H_n(x)$,

$$F_n(\xi) = [(q/\pi)^{1/2}/(2^n n!)]^{1/2}\exp(-q\xi^2/2)H_n(q^{1/2}\xi) . \tag{7}$$

The coefficients A_n and B_n in Eqs. (6a) and (6e) follow from the continuity of the potential ϕ and the normal component of the displacement field ($\epsilon\,\partial\phi/\partial\eta$) across the boundary ($\eta=\eta_0$). We will only need B_n:

$$B_n = -C_n\frac{\epsilon(w)-1}{\epsilon(w)V_0'U_0-V_0U_0'}U_iV_0V_0' , \tag{8}$$

where $V_0=V(n+\frac{1}{2},\sqrt{2q}\,\eta_0)$, $V_0'=dV_0/d\eta_0$, and similarly U_0 and U_0', and $U_i=U(n+\frac{1}{2},\sqrt{2q}\,\eta_i)$. The dispersion relation for the static modes is the result of equating the denominator in Eq. (8) to zero,[10] i.e.,

$$\epsilon(w)V_0'U_0-V_0U_0'=0 . \tag{9}$$

We seek the dissipative component of the force acting on the electron moving near the wedge surface. We neglect quantum recoil effects and assume that v is constant (i.e., the external charge acts as an infinite source of energy and momentum). The negative of the dissipative component of the induced force is the specific energy loss[14]

$$-\frac{dW}{dz} = \frac{e}{v}\frac{\partial\phi^{\text{ind}}}{\partial t}\bigg|_{\vec{r}=\vec{r}_i(t)} \tag{10}$$

and, from Eqs. (4), (6), (8), and (10), integration over q gives

$$-\frac{dW}{dz}=2ie^2\left[\frac{\pi}{v^3}\right]^{1/2}\sum_{n=0}^{\infty}\int_0^{\infty}dw\,w^{1/2}F_n^2(\xi_i)U_i^2V_0V_0'\frac{\epsilon-1}{\epsilon V_0'U_0-V_0U_0'} \tag{11}$$

(with $q=w/v$ replaced in the arguments of the functions U, V, and F_n). Now, the excitation probability is given by[15]

$$\frac{dW}{dz}=\int_0^{\infty}\frac{d^2P}{dz\,dw}\hbar w\,dw \tag{12}$$

and from Eqs. (11) and (12)

$$\frac{d^2P}{dz\,dw}=\frac{2e^2}{\hbar}\left[\frac{\pi}{v^3}\right]^{1/2}\sum_{n=0}^{\infty}w^{-1/2}F_n^2(\xi_i)U_i^2V_0V_0'\,\mathrm{Im}\left[\frac{\epsilon-1}{\epsilon V_0'U_0-V_0U_0'}\right], \tag{13a}$$

where Im($\cdots$) stands for the imaginary part. This expression holds for $\eta_i>\eta_0$. Writing $\epsilon=\epsilon_1+i\epsilon_2$, and assuming $\epsilon_2\ll\epsilon_1$, one gets in this particular case

$$\frac{d^2P}{dz\,dw}=\frac{4\pi e^2}{\hbar v^2}\sum_{n=0}^{\infty}F_n^2(\xi_i)U_i^2(V_0/U_0)\delta(\epsilon_1V_0'U_0-V_0U_0')\,. \tag{13b}$$

The zeros of the argument in the δ function provide[10] the electrostatic modes that the dielectric can sustain (eigenmodes w_n [Eq. (9)]). Writing Eq. (13b) as

$$\frac{d^2P}{dz\,dw}=\sum_{n=0}^{\infty}I_n\delta(w-w_n)\,, \tag{14}$$

the coefficient I_n gives the intensity of the nth mode w_n in the limit $\mathrm{Im}(\epsilon)\to 0$.

We consider now the case of a beam traveling through the wedge, but parallel to the edge. The analysis is quite similar to that described above and we only give the main differences and results. In Eq. (2) one replaces $\rho\to\rho/\epsilon$, and in Eq. (5b), $e\to e/\epsilon(w)$. The greater than/less than signs in the right-hand side terms of Eqs. (5a) and (5b) should also be reversed. The electrostatic potential inside the wedge now contains a further term due to the inhomogeneity in Poisson's equation, which the beam introduces. The potential inside the wedge is then given by

$$\phi^{\mathrm{in}}(\xi,\eta,q,w)=\sum_n A_n'F_n(\xi)V(n+\tfrac{1}{2},\sqrt{2q}\,\eta)+\phi^{\mathrm{inhom}}\,. \tag{15a}$$

This expression replaces Eq. (6a). The inhomogeneous solution ϕ^{inhom} is still given by Eq. (6c), and

$$A_n'=-C_n\frac{\epsilon-1}{\epsilon V_0'U_0-V_0U_0'}V_iU_0U_0'\,. \tag{15b}$$

The coefficient C_n entering Eq. (15b) is the same C_n in Eq. (6d), with the replacement $e\to e/\epsilon(w)$.

Now both terms in Eq. (15a) contribute to the specific energy loss of the beam traveling through the wedge. We only give the excitation probability, for $\eta_i<\eta_0$,

$$\frac{d^2P}{dz\,dw}=\frac{2e^2}{\hbar v^2}\sum_{n=0}^{\infty}F_n^2(\xi_i)V_i\left[\left[\frac{\pi v}{w}\right]^{1/2}\left[U_i-\frac{V_iU_0}{V_0}\right]\mathrm{Im}\left[-\frac{1}{\epsilon}\right]+\frac{V_iU_0}{V_0}\,\mathrm{Im}\left[\frac{-2}{\epsilon V_0'U_0-V_0U_0'}\right]\right]. \tag{16a}$$

With the assumption $\epsilon_2\ll\epsilon_1$, this expression becomes

$$\frac{d^2P}{dz\,dw}=\frac{4\pi e^2}{\hbar v^2}\sum_{n=0}^{\infty}F_n^2(\xi_i)V_i\left[\frac{1}{2}\left[\frac{\pi v}{w}\right]^{1/2}\left[U_i-\frac{V_iU_0}{V_0}\right]\delta(\epsilon_1)+\frac{V_iU_0}{V_0}\delta(\epsilon_1V_0'U_0-U_0'V_0)\right]. \tag{16b}$$

As expected, the excitation probability in Eqs. (16) contains terms corresponding to both the excitation of the bulk [the term $\mathrm{Im}(-1/\epsilon)$ or $\delta(\epsilon_1)$] and of the surface modes of the wedge. Therefore, if one wishes to probe the surface excitation field, without interference from the bulk modes, the probe has to be kept external to the wedge, as was done in the experiments.[1-3] One can calculate the specific energy loss from Eqs. (12) and (16).

Note in Eq. (9) that the variables v, η_0 determine the surface eigenmodes w_n that are excited for each n, but naturally these modes do not depend on the electron path (ξ_i,η_i). Also, for a fixed-electron beam energy and target geometry, the only variables in the excitation probability in Eqs. (13) and (16) are those determining the electron path (ξ_i,η_i).

It is instructive to compare Eqs. (13a) and (16a) with the excitation probability quoted by Marks[1] for an electron beam traveling parallel with a semi-infinite dielectric occupying the region $y<0$, and at a distance y_i from its surface which is[3,16,18]

$$\frac{d^2p}{dz\,dw}=\begin{cases}\dfrac{2e^2}{\pi\hbar w^2}\mathrm{Im}\left[\dfrac{\epsilon-1}{\epsilon+1}\right]K_0(2wy_i/v) & \text{for } y_i>0\,,\\[2ex] \dfrac{2e^2}{\pi\hbar w^2}\left\{\mathrm{Im}\left[\dfrac{-1}{\epsilon}\right]\left[\ln\left[\dfrac{k_cv}{w}\right]-K_0\left[\dfrac{2wy_i}{v}\right]\right]+\mathrm{Im}\left[\dfrac{\epsilon-1}{\epsilon+1}\right]K_0\left[\dfrac{2wy_i}{v}\right]\right\} & \text{for } y_i<0\,.\end{cases} \tag{17}$$

k_c is a cutoff wave number ($k_c \sim 0.1$ nm^{-1}).

In Eqs. (17) K_0 is the modified Bessel function of zeroth order. The surface energy-loss function $\mathrm{Im}[(\epsilon-1)/(\epsilon+1)]$, calculated from experimental data for the dielectric function for MgO,[17] did not predict the surface plasmon peak at 18 eV, which was, however, observed in the electron-energy-loss-spectrometry (EELS) data.[1] We will see in the following that this peak and other features of the experiment arise clearly from the parabolic model of the wedge.

Eguiluz and Maradudin[10] showed that in the limit of small wavelengths ($q \to \infty$) the dispersion relation of the edge modes, Eq. (9), coincides with the dispersion relation ($\epsilon = -1$) for surface plasmon modes bound to the plane interface between a dielectric medium and vacuum. Consequently, the surface energy-loss function in Eqs. (13a) and (16a) reduces to the surface energy-loss function in Eq. (17), $\mathrm{Im}[(\epsilon-1)/(\epsilon+1)]$, in the limit $\eta_0(2w/v)^{1/2} \to \infty$.

III. ANALYSIS AND COMPARISON WITH EXPERIMENT

We first briefly recall the principal results of the investigations carried out by Marks[1] and Cowley.[2]

(i) The overall intensity in the EELS spectrum (and therefore also the intensity of a given peak) decreases when the electron path goes *from* a lateral surface *to* the edge of the crystal (cf. Fig. 2 in Ref. 1 and Fig. 4 below).

(ii) For electron paths along a *lateral* surface, the intensity of a given peak first increases and then rapidly decreases exponentially as the beam-surface distance goes from inside to outside the wedge (cf. Fig. 3 in Ref. 1 and Fig. 5 below).

(iii) For electron paths both parallel to the lateral surface and along the edge, a surface plasmon at ~ 18 eV was observed, together with a strong enhancement of the low frequencies (in comparison with the spectrum for electron paths through the bulk, cf. Fig. 4 below). The 18-eV peak was attributed by Marks[1] to a genuine surface resonance, in contrast to Cowley's[2] interpretation of it as due to transition radiation.

Now we analyze the expressions (13) and (16) for the excitation probability. For fixed ξ_i and increasing η_i, the only factor in Eq. (13a) that varies then, for given n, is U_i^2. The function

$$U_i = U(n+\tfrac{1}{2}, (2w/v)^{1/2}\eta_i)$$

decreases exponentially for increasing η_i, for all n, and for $(2w/v)^{1/2}\eta_i \gg 1$ one has[13]

$$U_i^2 \sim \exp(-w\eta_i^2/v)[v/(2w\eta_i^2)]^{n+1} .$$

Since $\eta_i^2 = y_i + (y_i^2 + x_i^2)^{1/2}$, according to Eqs. (1), the probability of excitation decreases exponentially with distance as in Marks' experiment [cf. (ii) above]. In particular, for increasing distance away from the edge (along the y axis in Fig. 1), $\xi_i^2 = x_i = 0$, $\eta_i^2 = 2y_i$, and the y_i dependence in Eq. (13a) is

$$\frac{d^2P}{dz\,dw} \propto \sum_{n=0,2,4,\ldots}^{\infty} \exp(-2wy_i/v)[v/(4wy_i)]^{n+1} .$$

For comparison, Eq. (17) gives, for large $y_i > 0$,

$$\frac{d^2P}{dz\,dw} \propto \exp(-2wy_i/v)[v/(\pi w y_i)]^{1/2} .$$

In order to compare the experimental results with the predictions of Eqs. (13) and (16), one has to determine the parameters η_0 and (ξ_i, η_i). Figure 2 shows wedge profiles for different values of the parameter η_0. We are trying to model a sharp-edged wedge with a parabolic wedge, and in Marks' experiment[1] the electron beam travels at a distance ~ 2 nm from the edge or surface of the wedge. From this distance, the appearance of the parabolic wedges in Fig. 2 is nearly flat for values of $\eta_0^2 \gtrsim 10$ nm, and the wedge edge looks sharper for $\eta_0^2 \lesssim 1$ nm. The precise value of η_0 is not crucial in the calculations to follow, and we have chosen a value $\eta_0^2 = 0.5$ nm.

We have evaluated the excitation probabilities in Eqs. (13a) and (16a) with the complex dielectric function for MgO taken from experimental data,[17] and for an 80-keV electron beam as in the experiment.[1] Figure 3 shows the excitation probability for a beam traveling parallel to the edge of the wedge and in front of it, at a distance of 2 nm. Curve a corresponds to a wedge with well-defined edge, for a parameter $\eta_0^2 = 0.5$ nm, and b is the prediction for a nearly flat wedge, with $\eta_0^2 = 20$ nm. This latter case, which has been reduced by a factor of 5, is very similar to the flat-surface prediction in Eq. (17). Note that as the wedge parameter η_0^2 increases and the edge of the wedge flattens, the excitation probabilities increase in intensity, and also the peaks corresponding to larger $\hbar w$ values ($\gtrsim 16$ eV) become wider.

The resonance at $\hbar w \sim 18$ eV shown in Fig. 3 (curve a) was clearly observed in the experiments,[1,2] and is not so distinctly apparent in the predictions for the flat semi-infinite model of the wedge (cf. Ref. 1 or curve b in Fig. 3). Cowley[2] attributed this ~ 18-eV mode to transition radiation, but its origin as a genuine surface resonance is

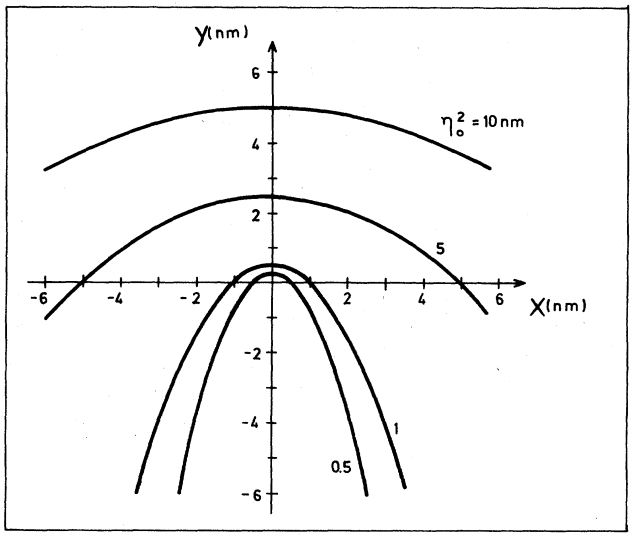

FIG. 2. Wedge profiles for different values of the parameter η_0^2. Note that in the experiments (Refs. 1 and 2), the beam passes at a distance ~ 2 nm from the wedge.

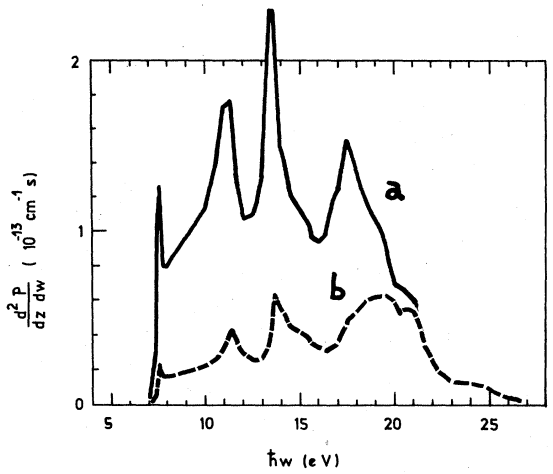

FIG. 3. Excitation probability of surface modes, Eq. (13a), for aloof electrons traveling in front of the edge of the wedge, at a distance ~ 2 nm. The parameter η_0^2 is (a) 0.5 nm, (b) 20 nm. The latter case resembles a flat semi-infinite wedge. The probability in curve b has been divided by a factor of 5. The electron beam energy is 80 keV. (For $\hbar\omega \gtrsim 21$ eV both curves overlap and the curve a has not been plotted for clarity.)

clear from the present model calculations.

For a wedge boundary defined by $\eta_0^2=0.5$ nm, Fig. 4 shows a comparison between the excitation probabilities of the wedge when the electron beam passes in front of the edge (curve E, which is the same as curve a in Fig. 3) or along one of its lateral surfaces (curve F). In both cases the distance from the beam to the wedge is ~ 2 nm, and in the interaction with the surface (curve F) the beam distance to the edge is taken to be ~ 20 nm. Also shown in Fig. 4 is the excitation probability (reduced by a factor of 4) for a beam traveling through the bulk of the wedge, along its symmetry plane (curve B), and at a distance ~ 20 nm from its edge. The results in Fig. 4 may be compared with the experimental findings in Fig. 2 of Ref. 1. The agreement both in the relative intensities of the bulk, face, and edge spectra and in the location of the peaks is very satisfactory. The details of the experiment are reproduced by our model calculations. For instance, in the F spectrum, the intensity of the ~ 18-eV peak is greater than the intensity of the ~ 13-eV peak. Also, the ~ 18-eV peak in the F spectrum shifts to ~ 22 eV in the B spectrum. The bulk plasmon for MgO is located at[17] $\hbar\omega_p \sim 22$ eV, as seen in Fig. 4.

As mentioned in (ii) above, Marks[1] also investigated the excitation probability of the wedge for electron beam positions ranging from ~ 10 nm with respect to the wedge surface, but *inside* the wedge, up to ~ 10 nm *outside* the dielectric wedge surface. The beam path in the experiment was far from the edge of the wedge, and the dimensions of the cubic crystal were ~ 100 nm. We have evaluated the corresponding expressions, (13a) and (16a), for $\eta_0^2=20$ nm, $\xi_i^2 \simeq 80$ nm, and $\eta_i^2 \simeq 20$ nm, and the results are shown in Fig. 5. In agreement with the experimental results [Fig. 3 in Ref. 1, cf. also point (ii) above], the excitation function decays exponentially with distance,

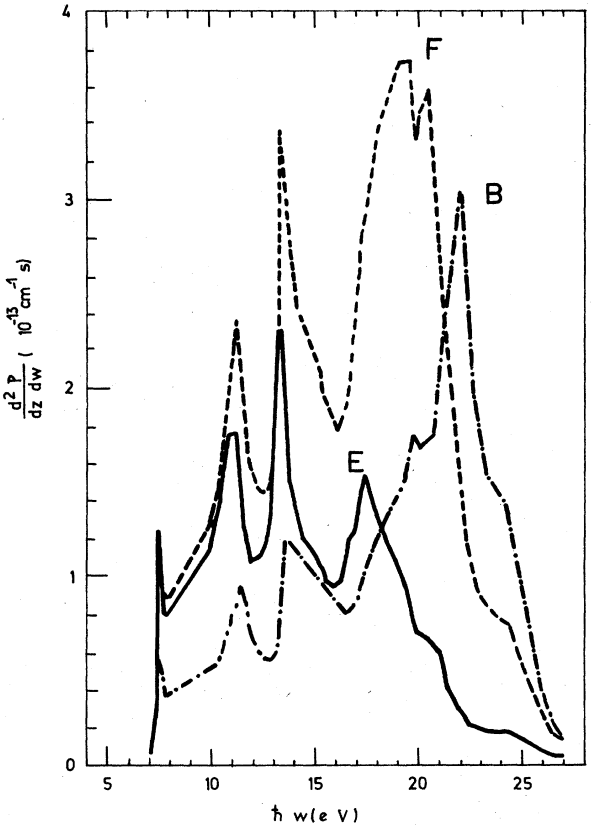

FIG. 4. Excitation probability of surface and bulk modes, Eqs. (13a) and (16a), for electrons traveling (E) along the edge, at a distance of 2 nm from the edge; (F) along a lateral surface, at a distance of 2 nm from it; and (B) through the bulk of the wedge, along the symmetry plane and at a distance ~ 20 nm from the edge. The spectrum (B) has been divided by a factor of 4. The wedge parameter is $\eta_0^2=0.5$ nm and the electron beam energy is 80 keV.

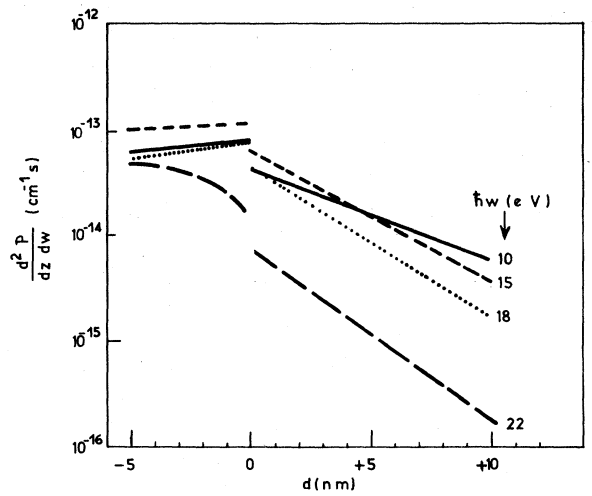

FIG. 5. Excitation probability, for given modes $\hbar\omega$, Eqs. (13a) and (16a), for electron beam paths at varying distance d from the lateral surface of the wedge. The electron paths are far away from the edge, ($\eta_i^2 \simeq 20$ nm) and range from inside ($d<0$) to outside ($d>0$) the wedge. Wedge parameter $\eta_0^2=20$ nm. Electron energy is 80 keV.

the slope being larger the larger the energy window $\hbar w$. The relative intensities of the different curves are also in agreement with the experimental findings, the curve for $\hbar w = 10$ eV crossing the other curves shown in Fig. 5. There is only some discrepancy in the region close to the surface (distance ~ 0 nm in Fig. 5). In the experiment the transition from inside to outside the wedge is broader than Fig. 5 shows. One should note, however, that our model calculations assume a δ function for the cross-sectional area of the beam, whereas the experimental value of this cross section was rather large, ~ 2 nm. We recall also that the spectrometer resolution in Marks'[1] experiment is 3 eV. It is interesting to note, finally, that whereas the expression for the excitation probability of an electron traveling inside the wedge and parallel to the plane boundary, Eq. (17), contains a cutoff wave vector[18] and, furthermore, the function K_0 is divergent for zero argument,[13] none of these features arise in the present calculations based on a parabolic-function expansion of the electrostatic potential. This expansion is rapidly convergent for beam paths in front of the edge (i.e., $\xi_i = 0$), and, furthermore, in this case, the odd-n terms are identically zero because the Hermite polynomials in Eq. (7) cancel. For electron beam positions far away from the edge, we have taken up to eight terms in the expansion in Eqs. (13) and (16).

IV. FINAL REMARKS

We have investigated here the case of a beam traveling parallel to the edge of a parabolic wedge both in vacuum and through the medium. Other configurations, like beam trajectories at constant z, trajectories intersecting the tip of the wedge, or reflecting at the lateral surface, may also be of interest in the analysis of the experiment. Note also that the experiment has been performed with a relatively broad probe, ~ 2 nm in diameter, which is comparable to the distance from the beam to the wedge whereas the model calculations developed in this paper assume a δ function for the STEM probe. This is only a crude approximation. In particular, also, we are neglecting diffraction by the probe inside the bombarded wedge. When the approximation of the beam cross section as a δ function is not appropriate, one can convolute the excitation probabilities derived in this paper with the appropriate beam profile.

Cowley[2] finds features in the EELS spectrum which seem to correlate with the length of the crystal in the beam direction. Since the crystal is assumed to be infinite in the beam direction in the present treatment, we cannot look into those features, which have been discussed in Ref. 18.

We have analyzed the electron-wedge interaction in the electrostatic limit. The electron beam energy (~ 100 keV) is large enough that one may worry about the effect of retardation on the theoretical predictions. This is currently being investigated.[19]

Finally, let us mention that the expressions derived for the excitation probability in Eqs. (13b) and (16b) can be used to analyze experiments where a detailed knowledge of the complex dielectric function is not available, and one may resort to a free-electron-gas expression for $\epsilon(w)$, for instance.

ACKNOWLEDGMENTS

Comments by Dr. A. Howie on a preliminary version of this manuscript are appreciated. Partial support from the U.S.—Spanish Joint Committee for Scientific and Technological Cooperation, the Spanish Comisión Asesora de Investigación Científica y Técnica (CAICYT), and travel grants from The British Council are acknowledged. This research was also supported in part by the Office of Health and Environmental Research, U. S. Department of Energy, under Contract No. W-7505-eng-26 with the Union Carbide Corporation and partly by the Deputy for Electronic Technology, U. S. Air Force Systems Command, under U. S. Department of Energy Interagency agreement No. DOE-40-226-70.

[1] L. D. Marks, Solid State Commun. **43**, 727 (1982).
[2] J. M. Cowley, Surf. Sci. **114**, 587 (1982); Phys. Rev. B **25**, 1401 (1982).
[3] D. I. Wheatley, A. Howie, and D. McMullan, EMAG Conference Surrey, 1983 (unpublished).
[4] J. P. Muscat and D. M. Newns, Surf. Sci. **64**, 641 (1977).
[5] W. R. Smythe, *Static and Dynamic Electricity* (McGraw-Hill, New York, 1969).
[6] L. Dobrzynsky and A. A. Maradudin, Phys. Rev. B **6**, 3810 (1972).
[7] L. D. Davis, Phys. Rev. B **14**, 5523 (1976).
[8] J. Sánchez-Dehesa and F. Flores, Solid State Commun. **35**, 815 (1980).
[9] A. A. Maradudin, in *Festkorperprobleme (Advances in Solid State Physics)*, edited by J. Treusch (Vieweg, Braunschweig, 1981), Vol. XXI, p. 25.
[10] A. Eguiluz and A. A. Maradudin, Phys. Rev. B **14**, 5526 (1976).
[11] A. D. Boardman, G. C. Aers, and R. Teshima, Phys. Rev. B **24**, 5703 (1981).
[12] P. Morse and H. Feshbach, *Methods of Theoretical Physics* (McGraw-Hill, New York, 1953), pp. 501—502. Also J. A. Stratton, *Electromagnetic Theory* (McGraw-Hill, New York, 1941), p. 54.
[13] *Handbook of Mathematical Functions,* edited by M. Abramowitz and I. A. Stegun, National Bureau Standards Applied Mathematical Series, No. 55 (U.S. G. P. O., Washington, D.C., 1972), pp. 686 and 774.
[14] R. Nuñez, P. M. Echenique, and R. H. Ritchie, J. Phys. C **13**, 4229 (1980).
[15] R. H. Ritchie, Phys. Rev. **106**, 874 (1957).
[16] R. H. Ritchie (unpublished).
[17] D. M. Roessler and W. C. Walker, Phys. Rev. **159**, 733 (1967).
[18] A. Howie, Ultramicroscopy **11**, 141 (1983).
[19] R. H. Ritchie, A. Howie, A. Gras-Marti, and R. Garcia-Molina (unpublished).